Propulsion and Power Research 2014;3(3):107–120

HOSTED BY

ELSEVIER

http://ppr.buaa.edu.cn/

Propulsion and Power Research

www.sciencedirect.com


ORIGINAL ARTICLE

# Buoyancy effect on heat transfer in rotating smooth square U-duct at high rotation number


**Yang Li[a,*], Guoqiang Xu[a], Hongwu Deng[a], Shuqing Tian[b]**

[a]*National Key Laboratory of Science and Technology on Aero-Engine Aero-Thermodynamics & Collaborative Innovation Center of Advanced Aero-Engine, Beihang University, Beijing 100191, China*
[b]*R&D Center Dept of Discipline Engineering, AVIC Commercial Aircraft Engine Co., Ltd., Shanghai 201108, China*

Received 30 October 2013; accepted 3 July 2014
Available online 1 October 2014

**KEYWORDS**

Buoyancy effect;
Heat transfer;
Wall temperature ratio;
Rotating U-duct;
High rotation number

**Abstract** The buoyancy effect on heat transfer in a rotating, two-pass, square channel is experimentally investigated in current work. The classical copper plate technique is performed to measure the regional averaged heat transfer coefficients. In order to perform a fundamental research, all turbulators are removed away. Two approaches of altering Buoyancy numbers are selected: varying rotation number from 0 to 2.08 at Reynolds number ranges of 10000 to 70000, and varying inlet density ratio from 0.07 to 0.16 at Reynolds number of 10000. And thus, Buoyancy numbers range from 0 to 12.9 for both cases. According to the experimental results, the relationships between heat transfer and Buoyancy numbers are in accord with those obtained under different rotation numbers. For both leading and trailing surface, a critical Buoyancy number exists for each *X/D* location. Before the critical point, the effect of Buoyancy number on heat transfer is limited; but after that, the Nusselt number ratios show different increase rate. Given the same rotation number, higher wall temperature ratios with its corresponding higher Buoyancy numbers substantially enhance heat transfer on both passages. And the critical exceed-point that heat transfer from trailing surface higher than leading surface happens at the same Buoyancy number for different wall temperature ratios in the second passage. Thus, the stronger buoyancy effect promotes heat transfer enhancement at high rotation number condition.



## 1. Introduction

Current advanced turbine engines operate in the abominable environment with extreme high temperature, which is

*Corresponding author: Tel.: +86 10 82339665.
E-mail address: buaalzw@gmail.com (Yang Li).

Peer review under responsibility of National Laboratory for Aeronautics and Astronautics, China.


http://dx.doi.org/10.1016/j.jppr.2014.07.001

## Nomenclature

| | |
|---|---|
| $A$ | area (unit: $m^2$) |
| $Buo$ | rotational buoyancy parameter, $Buo=(\Delta T/T)Ro^2(r/D)$ |
| $C_p$ | specific heat at constant pressure (unit: kJ/(kg · K)) |
| $D_h$ | hydraulic diameter (unit: m) |
| $h$ | heat transfer coefficient (unit: W/($m^2$ · K)) |
| $\dot{m}$ | mass flow rate (unit: kg/s) |
| $Nu$ | regionally averaged Nusselt number, $Nu=hD/\lambda$ |
| $Pr$ | Parndtl number |
| $P$ | pressure (unit: Pa) |
| $Q$ | heat energy (unit: W) |
| $R$ | the resistance of each heater (unit: Ω) |
| $r$ | mean rotating radius (unit: m) |
| $r/D_h$ | rotational radius ratio |
| $Re$ | Reynolds number, $Re=\rho V_{in}D/\mu$ |
| $Ro$ | rotation number, $Ro=\Omega D/U_{in}$ |
| $T$ | temperature (unit: K) |
| $TR$ | wall temperature ratio, $TR=(\overline{T}_w-T_{in})/\overline{T}_w$ |
| $U$ | mean average velocity (unit: m/s) |
| $X$ | electromagnetic energy density (unit: J/$m^3$) |

### *Greek letters*

| | |
|---|---|
| $\alpha$ | wall-to-environment heat loss coefficient (unit: W/K) |
| $\Omega$ | rotation speed (unit: rpm) |
| $\lambda$ | thermal conductivity (unit: W/(m · K)) |
| $\rho$ | density (unit: kg/$m^3$) |
| $\mu$ | molecular dynamic viscosity (unit: kg/(m · s)) |

### *Subscripts*

| | |
|---|---|
| *all* | all |
| *b* | bulk |
| *e* | environment |
| *i* | the number of the measured point in *X* direction |
| *in* | inlet for heated channel |
| *loss* | loss |
| *net* | net |
| *out* | outlet |
| *s* | stationary |
| *x* | local parameter |
| *w* | wall |

far above the permissible metal temperatures. In order to guarantee their safe operation, turbine blades need to be cooled by both internal and external cooling techniques. Over the past decade, research on gas turbine blade internal cooling has progressed considerably and many works have been systematically reviewed by Han et al. [1–3].

The current paper focuses on the heat transfer in rotating U-duct, which is a basic unit of rotating serpentine passage in the middle internal cooling section of turbine blades. In order to provide a more fundamental study, all turbulators in real internal cooling channels are removed, and thus, smooth square channel is selected in this research. In general, the effective factors on flow and heat transfer in these kinds of rotating channels can be separated into two parts: (1) geometrical factors: such as channel orientation, channel aspect ratio, channel entrance form, a 180-deg turn, and turbulator arrangements, etc. (2) physical factors: such as the strength of inertia force, rotation induced Coriolis and centrifugal buoyancy forces, and thermal boundary conditions, etc. Among all these important factors, this paper focus on the combined effect of rotation induced Coriolis and centrifugal buoyancy forces, and thermal boundary conditions on heat transfer in rotating U-duct.

It has been demonstrated that rotation can significantly alter the local heat transfer in a rotating internal cooling channel due to the presence of the rotational induced Coriolis and centrifugal buoyancy forces. Substantially, the interaction of rotation induced Coriolis and buoyancy effects multiplies the complexity of rotating heat transfer studies. And thus, flow in rotating channels becomes extraordinary complicated and three-dimensional. Luckily, many investigations on rotating U-ducts have been published by many previous works over the past two decades [4–17].

## 1.1. Effect of geometrical factors

The coolant flow in the rotating channel is complex and affected by multiple factors. The 180-deg turn in the multi-pass channels, channel orientations, channel aspect ratio and channel entrance form all affect the level of heat transfer enhancement in a rotating smooth channel.

### 1.1.1. 180-deg turn

Han et al. (1988) [4] concentrated on the heat transfer in the 180-deg turn region. Results indicated that the 180-deg turn had positive effect on heat transfer in the turn and downstream. Yang et al. (1992) [5] and Mochizuki et al. (1994) [6] studied heat transfer in rotating multi-pass smooth square channels vie copper plate heating technique. They concluded that the flow exhibited strong three dimensional structure in the 180-deg bends and a significant enhancement in heat transfer performance could be observed at all sharp turns.

### 1.1.2. Channel orientations

Johnson et al. (1994) [7] reported their investigations of smooth serpentine channels with channel orientation angles of 0 and 45-deg, respectively. They found that the effects of the Coriolis and buoyancy forces on heat transfer are decreased when the channel has an angle to the axis of rotation. And thus, the rotation effect on heat transfer diminished and the heat transfer difference between leading and trailing surface was reduced. In 2009 and 2010, Huh et al. [8,9] investigated heat transfer in rotating two-pass rectangular channel with channel orientation angles of 0 and 45-deg at high rotation number. Their observed that channel

orientation could enhance heat transfer on leading surface in the first passage at high rotation numbers.

#### 1.1.3. Channel aspect ratio

Azad et al. (2002) [10] studied effect of channel aspect ratio on heat transfer for a 2:1, two-pass channel. Compared with square channel, heat transfer in 2:1 channel decreased on the leading surface while increased on the trailing surface in the first radially outward passage, and the opposite occurred in the second radially inward passage. Fu et al. (2005) [11] confirmed this result in a rotating two-pass smooth channel with channel aspect ratio of 1:2 and 1:4. They also showed that rotation had a relatively small effect in the second pass of the 1:2 and 1:4 channels compared with square channel.

#### 1.1.4. Channel entrance form

It is well accepted that the effect of a developing flow entrance is markedly different from fully developed flows, due to the thin boundary layer. Wright et al. (2005) [12] conducted experiments in channels with three different entrance geometries. They found that the entrance condition will enhance heat transfer. And they also included that the effect of entrance weakens as rotation number increases. Huh et al. (2009) [8] investigated a sudden expansion from a circular tube to the rectangular cross section of the channel. They pointed out heat transfer is dominated by the entrance until the large Buoyancy number.

### 1.2. Effect of physical factors

In rotating internal cooling passage, the rotation effect on heat transfer derives from the Coriolis and centrifugal forces. Generally, two dimensionless parameters (rotation number and Buoyancy number) are employed to quantify the rotational effect. The conventional perspective of correlating heat transfer in rotating channel is to consider the variation of rotation number. However, it is worthwhile to develop different nondimensional parameters to correlate rotating effects on heat transfer.

#### 1.2.1. Rotation number

Wagner et al. (1991) [13,14] systematically showed heat transfer differences in a rotating four-pass smooth channel. They concluded that the rotation induced Coriolis force has a positive effect on heat transfer of trailing wall but negative effect on leading wall with radially outward flow. And in the second passage, the leading surface with radially inward flow experienced heat transfer enhancement while the trailing surface decreased due to the reversal of the Coriolis force. In 2013, Deng et al. [15] conducted extensive experimental investigations on heat transfer in a rotating smooth U-duct at high rotation numbers. They correlated heat transfer with critical rotation number ($Ro_c$) and dimensionless location ($X/D$) on the leading wall of first passage. And they found that heat transfer coefficients on trailing wall were evidently higher than leading wall at high rotation numbers in the second passage.

#### 1.2.2. Inlet density ratio

The inlet density ratio has a significant influence on heat transfer over a range of rotation numbers. According to the results shown by Hajek et al. (1986) [16], inlet density ratio had a larger effect on the pressure side than the suction side and diminished its influence in the second passage. The same finding was also shown by Wagner et al. (1991) [13,14]. They concluded that the increasing inlet density ratio enhanced the Nusselt number ratio for both pressure and suction side surface.

#### 1.2.3. Buoyancy number

The Buoyancy number combines the effects of density ratio, rotation number, and a geometric configuration parameter (radius ratio). Huh et al. (2010) [9] showed that regional averaged Nusselt number ratios are affected by variations of the Buoyancy number in the same approximate qualitative manner as when the rotation number changes. They concluded that Nusselt number ratios increase with Buoyancy number on the passage pressure side and decrease with Buoyancy number on the passage suction side in the radially outward flow. And the converse is generally true.

However, most investigations on the correlation between Nusselt number and Buoyancy number are varying rotation number, and fewer concerns are concentrated on the combined effects of rotation numbers and density ratios. Moreover, most previous works are performed at relatively low rotation number and heat transfer characteristics at high rotation number are hardly reported by open literatures. While increasing the range of the rotation number and buoyancy parameter is very important for gas turbine engineers to utilize these parameters in their analysis of heat transfer under rotating conditions, the current study extends the work of Deng et al. [15,17] by considering the effects of buoyancy parameter at high rotation number. And the objectives of current work can be summarized as follow:

By extending the range of the rotation number and Buoyancy number to 0.0–2.08 and 0.0–12.9, respectively, investigate the effect of buoyancy parameter on heat transfer in rotating smooth U-duct. Also, the combined effects of rotation number and density ratio on heat transfer are investigated to explain the critical exceed-point in the second passage. Two approaches of altering Buoyancy numbers are selected: varying rotation number from 0 to 2.08 at Reynolds number ranges of 10000 to 70000, and varying inlet density ratio from 0.07 to 0.16 at Reynolds number of 10000.

## 2. Experimental material

### 2.1. Experimental facilities

The rotating rig (as shown in Figure 1) consists of three main modules: the main support module, temperature

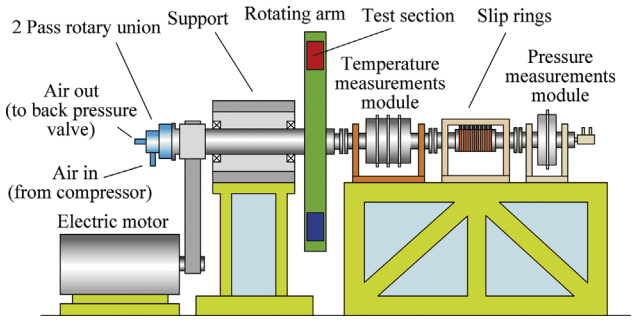


**Figure 1** Rotating facility.

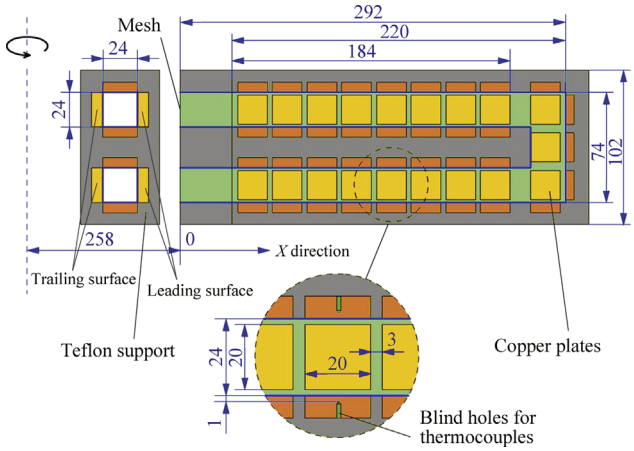


**Figure 2** Test section (unit: mm).

**Table 1** Ranges of the experimental variables.

| Variables | Test ranges (Different Reynolds numbers) | Test ranges (Different wall temperatures) |
|---|---|---|
| Rotation speed/rpm | 0–1000 | 0–1000 |
| $D_h$/mm | 24 | 24 |
| $R_{ave}/D_h$ | 17.25 | 17.25 |
| Back pressure/atm | about 5 | about 5 |
| Density ratio | 0.16 | 0.07, 0.11, 0.16 |
| $Re/10^{-3}$ | 10–70 | 10 |
| *Ro* | 0–2.08 | 0–2.08 |
| *Buo* | 0–12.9 | 0–12.9 |

measurements module, slip rings module. All these three modules are connected by the standard interface and are supported by bearings independently. Thus, each module can be replaced and upgraded in convenience.

(1) The main support module consists of two-pass rotary union, rotating arm and its consolidated support. The test section is placed at the top of the rotating arm with the maximum rotating diameter of 1.3 m. (2) In temperature measurements module, seventy-eight T-type thermocouples are applied in test section to measure the temperatures (seventy-five for wall temperature, two for inlet and outlet air temperature, and one for environment temperature). The analog

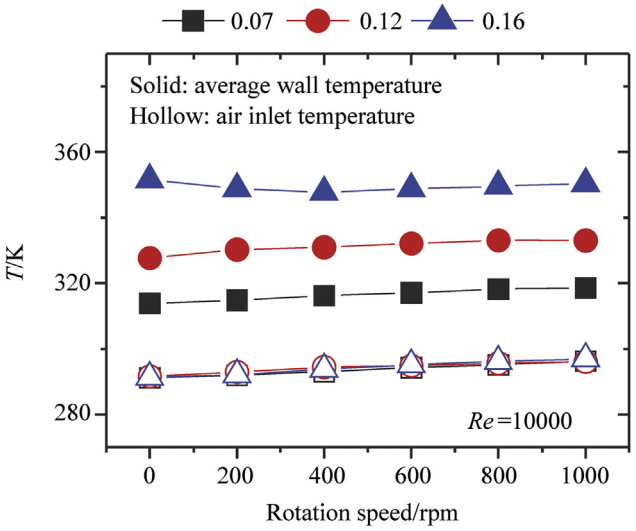


**Figure 3** Air inlet temperature and average wall temperature for $Re = 10000$.

signals of the thermocouples are converted into digital ones under rotating condition before transmitted to the non-rotating facilities by slip rings. All the cold ends of these thermocouples are placed in a rotating cavity isolating from hot parts. And the temperatures in this cavity can be relatively constant and even and is measured by several DS18B20 chips. (3) In slip rings

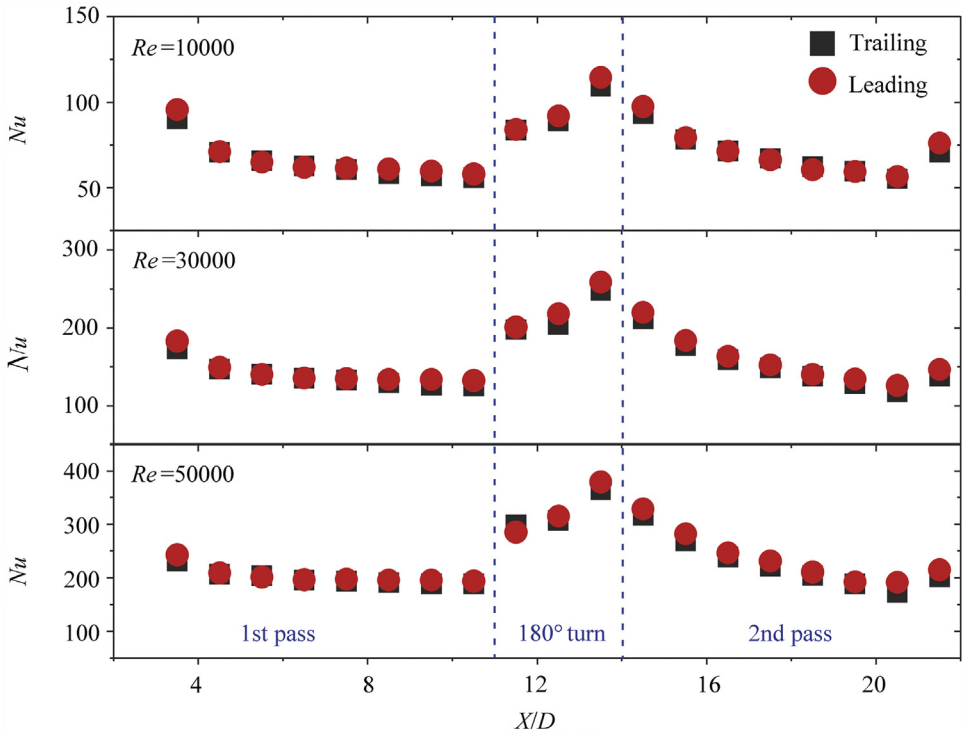


**Figure 4** Nusselt number distributions for different Reynolds number in stationary.

modules, only four slip rings (two for AD-chips power supply and two for data transmission) are required to measure hundreds of temperatures.

In current study, the flow channel is perpendicular to the ground at stationary. All the experimental conditions are operated at the same state. A FCI thermal flow-meter is placed before the coolant transported into the rotating test section to measure the mass flow. The absolute pressure of the entire system can be maintained up to 5 atm and the maximum rotation speed is 1000 rpm.

## 2.2. Test section

The dimensions of U-duct are shown in Figure 2 and experimental variables are shown in Table 1. The hydraulic diameter of this square channel is 24 mm. The entire channel has a height of 292 mm, including three parts: (1) 184 mm long heated straight section where the regional averaged heat transfer coefficients are measured, (2) 72 mm long unheated square duct before/ after the heated section which ensures better inlet/outlet boundary conditions, (3) 36 mm long 180 degree turn section which is also heated. The average radius of the channel is 414 mm. In addition, there is a 20 mm long honeycomb inlet section and a mesh before the channel inlet. And the location after the mesh is set to be $X=0$.

As shown in Figure 2, the U-duct channel is assembled by several Teflon frameworks. Seventy-five 20 mm × 20 mm copper plates are embedded into the Teflon framework to measure the regional averaged heat transfer coefficients. Eight coppers on each wall in the stream-wise direction in

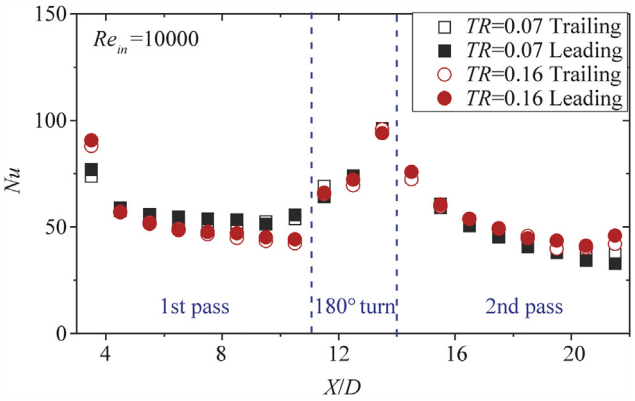


**Figure 5** Nusselt number distributions for different *TR* in stationary.

each straight leg with 3 mm interval for each copper to its neighbour in stream-wise direction and 2 mm distance to the neighbor wall in span-wise direction. In the 180-deg turn, eleven coppers are arranged in three surfaces: five coppers for outer surface, and three coppers for leading and trailing surface respectively. Each copper is heated by a small film heater independently. All the heaters have the same resistances and connected in series so that the overall thermal boundary is nearly constant heat flux. The wall temperature on each copper plate is measured by thermo-couple placed in the blind hole on the back of each copper plate. The air inlet temperature and average wall temperature for $Re=10000$ are shown in Figure 3. It is clearly seen that the temperature levels for different test condition is rather stable. And the whole test section is enveloped in a

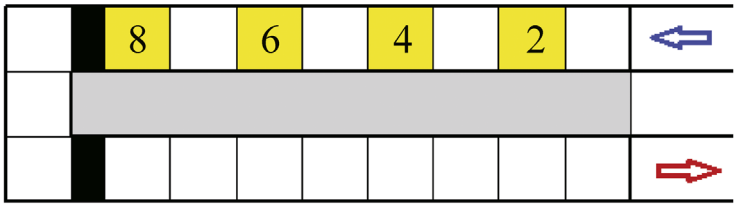


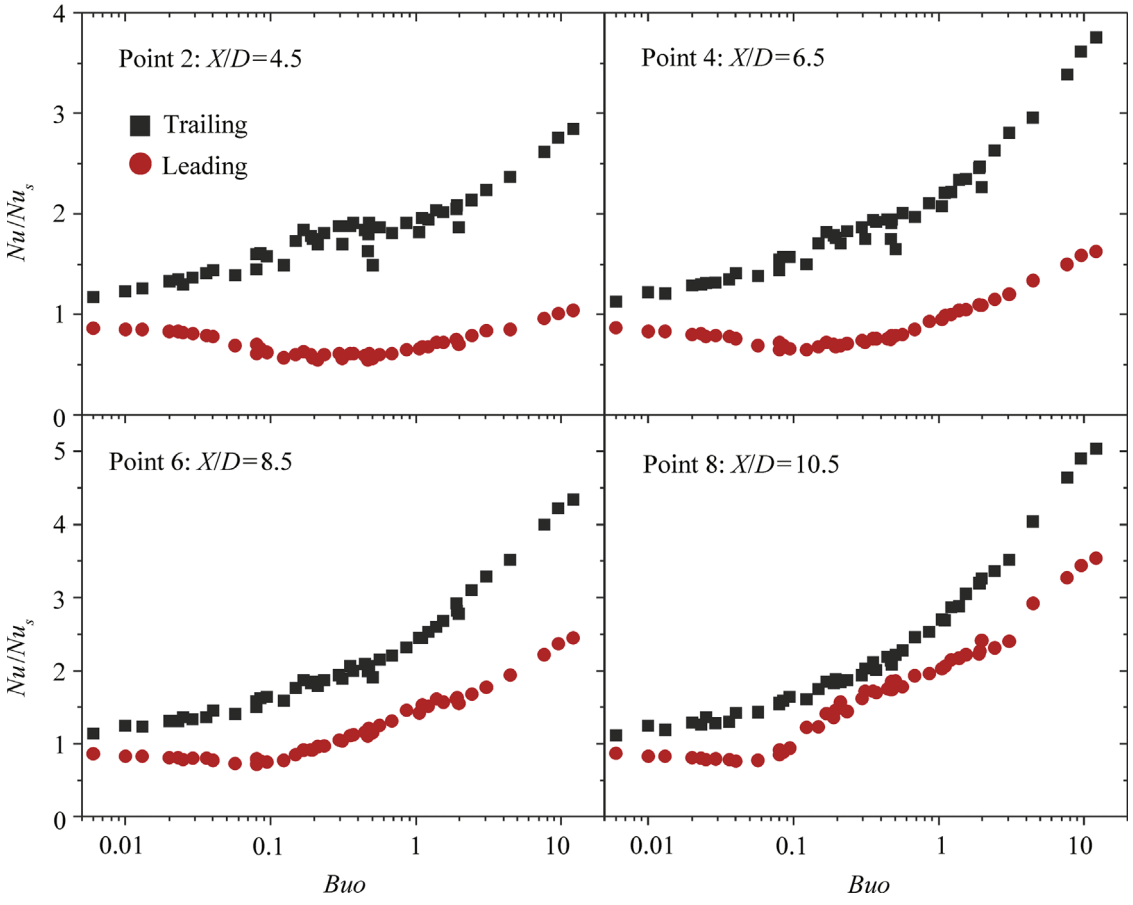


**Figure 7** Effect of Buoyancy number on Nusselt number ratios at each location in first passage.

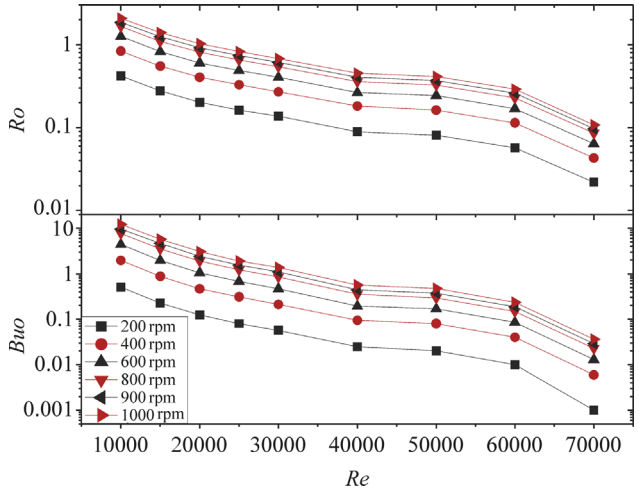


**Figure 6** The ranges of *Ro* and *Buo* at different Reynolds numbers.

cylinder pressure vessel to reach higher rotation number with the absolute pressure of up to 5 atm.

## 3. Data reduction

In current study, the regional average heat transfer coefficients are calculated using the net heat fluxes from the heated copper plate, the projected surface area of each copper plate, wall temperatures and local bulk temperatures.

$$h_i = \frac{Q_{net,i}}{A_i(T_{w,i} - T_{b,i})} \tag{1}$$

The energy generated by each film heater can be divided into two parts: the energy taken away by the coolant $Q_{net}$ and the energy dissipated into the environment $Q_{loss}$. Given

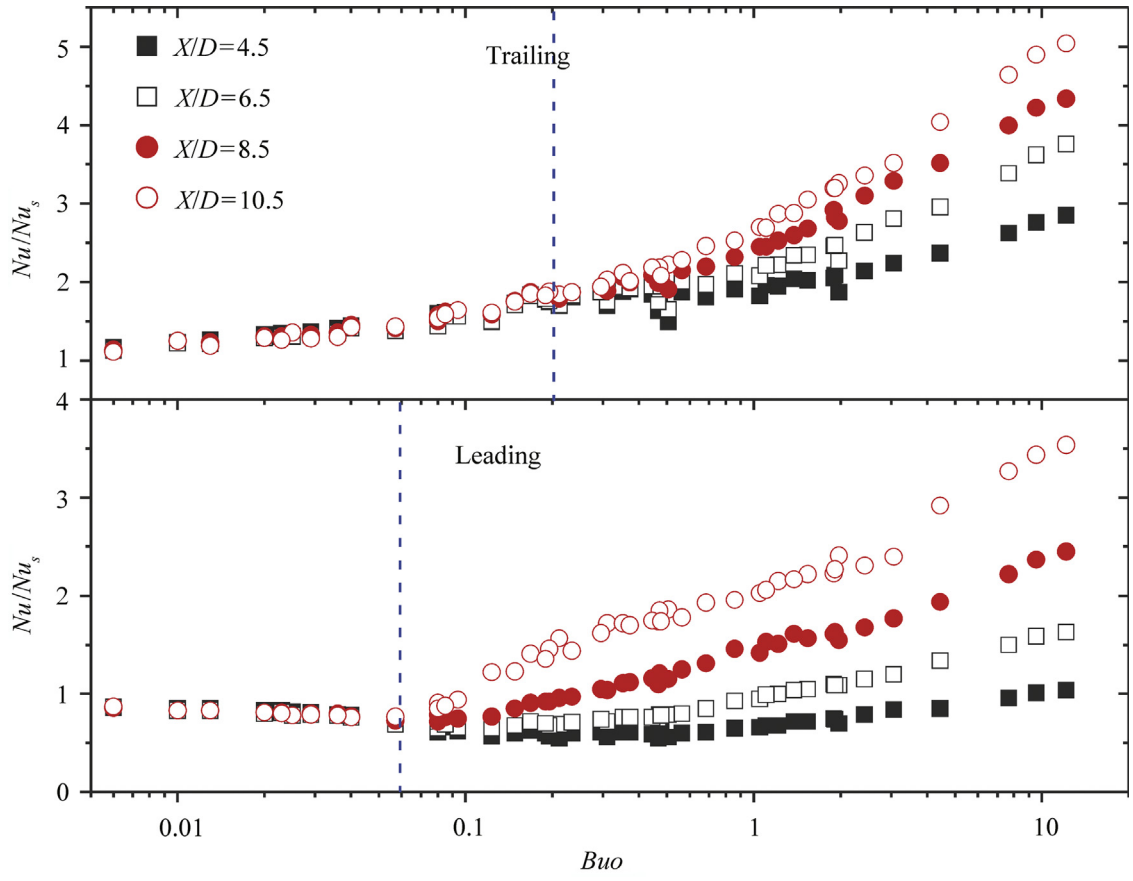


**Figure 8** Effect of Buoyancy number on Nusselt number ratios at each surface in first passage.

that the heat loss is hard to eliminate, a heat loss calibration test is performed for each rotational speed, including stationary.

$$Q_{all} = I^2R = Q_{net} + Q_{loss} = hA(T_w - T_b) + \alpha(T_w - T_e) \quad (2)$$

Heat loss coefficients, which are based on one-dimensional conduction theory, are employed to quantify the heat loss for both stationary and rotating conditions by heat loss experiments, in which the channel is heated but fulfilled with insulation. When the wall temperatures level off, all the energy generated by heaters dissipates into the environment, so seventy-five heat loss coefficients are obtained for each rotational speed. In current study, the percentage of heat loss varies from 3.8% ($Re$=70000, rotation speed=0) to 17.0% ($Re$=10000, rotation speed=1000 rpm).

$$\alpha_i = \frac{Q_{loss,i}}{(T_{w,i} - T_e)} = \frac{I^2R_i}{(T_{w,i} - T_e)} \quad (3)$$

Thus, the local averaged heat transfer coefficients and Nusselt number can be calculated as followed:

$$h_i = \frac{I^2R_i - Q_{loss,i}}{A_i(T_{w,i} - T_{b,i})} = \frac{I^2R_i - \alpha_i(T_{w,i} - T_e)}{A_i(T_{w,i} - T_{b,i})} \quad (4)$$

The local bulk temperature is calculated by local energy balance method which is shown by following equation:

$$T_{b,x} = \frac{T_{in,x} + T_{out,x}}{2} = T_{in,x} + \frac{1}{2}\frac{\sum_{span-wise} Q_{net}}{\dot{m}_x C_p} \quad (5)$$

$$Nu_i = \frac{h_i D_h}{\lambda} \quad (6)$$

Beyond the geometry concerns, the inertia force, Coriolis force and centrifugal buoyancy force are three most important factors in rotating cooling channel. Hence, it is believed that three dimensionless numbers are responsible to Nusselt number.

$$Nu_i = f\left(\frac{X_i}{D_h}, Re, Ro, Buo\right) \quad (7)$$

in which,

$$Re = \frac{\rho U D_h}{\mu} = \frac{\dot{m} D_h}{A\mu} \quad (8)$$

$$Ro = \frac{\Omega D_h}{U} \quad (9)$$

$$Buo = \frac{(\overline{T}_w - T_{in})}{\overline{T}_w} Ro^2 \frac{r}{D_h} \quad (10)$$

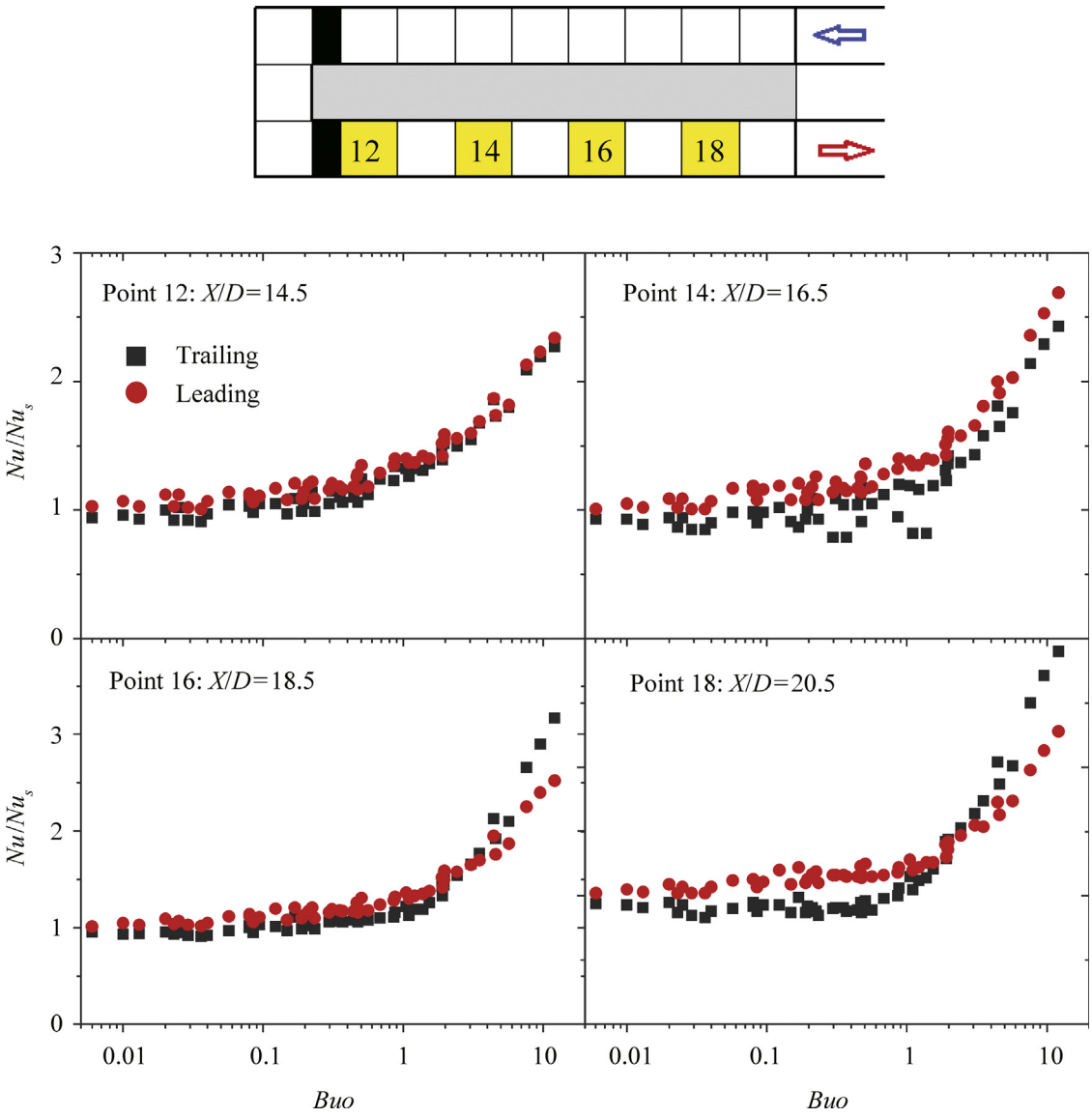


**Figure 9** Effect of Buoyancy number on Nusselt number ratios at each location in second passage.

Here the mean rotational radius is defined as the length between the middle of the channel and the rotating axis. The Dittus-Boelter/McAdams correlation for heating ($T_{w,x} > T_{b,x}$) is used in current study to provide a basic of comparison. In order to estimate the rotation effect on heat transfers, the parameter $Nu/Nu_s$ (rotation-to-stationary ratio) is introduced in the following comparison:

$$\frac{Nu_i}{Nu_s} = f\left(\frac{X_i}{D_h}, Ro, Buo\right) \tag{11}$$

All air properties are taken based on the channel average bulk air temperature with a Prandtl number ($Pr$) of 0.71. An uncertainty analysis was performed based on the method described by Kline and McClintock [18]. The uncertainty of Reynolds number and inlet rotation number are 2.6% and 3.3% of the presented data. Moreover, the maximum uncertainty of the Buoyancy number is 6.0%. The uncertainty of Nusselt number varies from 3.5% to 19.7%. Systematic errors and random effects are not included in this process, and all the uncertainty analysis only concerns limited precision.

## 4. Results and discussion

### 4.1. Non-rotating results

Before the discussion of the rotational effects, non-rotating validations are necessary to guarantee the reliability of the experimental data.

Figure 4 presents Nusselt number ratios distribution on leading and trailing surface at three Reynolds number in stationary. The trends of stream-wise Nusselt number variations are similar for different Reynolds numbers. In the first passage, because the length of the entrance is too

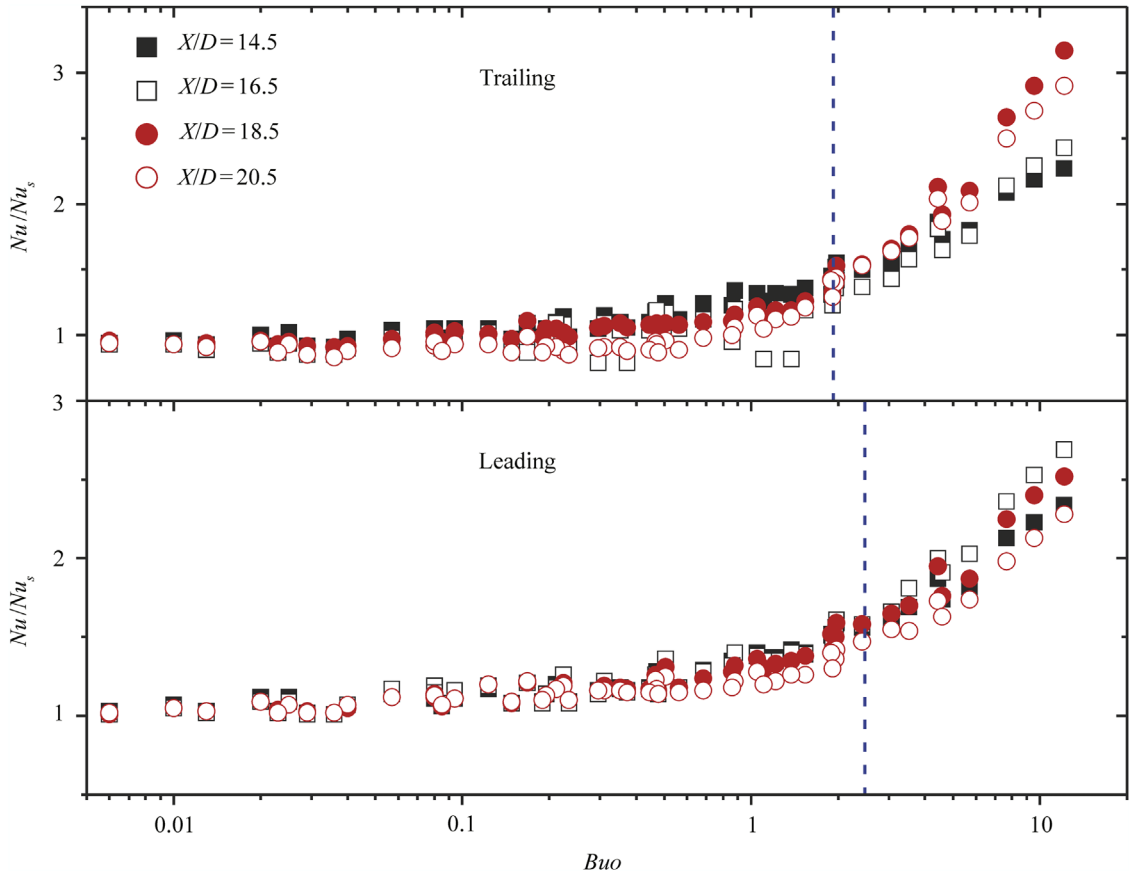


**Figure 10** Effect of Buoyancy number on Nusselt number ratios at each surface in second passage.

short to afford a fully developed fluid flow, the heat transfer near the inlet is significantly enhanced by the entrance effect due to the boundary layer is thin. As the coolant travels to the downstream, Nusselt number slightly reduce to a constant value for both Reynolds number.

In the 180-deg sharp turn, heat transfers are extremely high because of the impingement and turning effect. The highest heat transfer point happens at the location of $X/D=13.5$, the very beginning of the second passage. After the 180-deg turn, heat transfer decrease in stream-wise direction, but recovers a little bit at the end of the second passage due to the outlet effect.

The non-rotating Nusselt number distributions for $TR=0.07$ and $TR=0.16$ on leading and trailing surface are shown in Figure 5. In the first passage, heat transfer in $TR=0.16$ is weaker than $TR=0.07$ in the flow direction. The underlying mechanisms can be accounted for the decrease of the local Reynolds numbers which quantify the ratio between inertial forces and viscous forces inside the boundary layer. It is the combined effects of local temperature on density, velocity and viscosity that together contributed to the decrease of heat transfer in higher $TR$ conditions. While in the 180-deg sharp turn, heat transfers are almost the same which are predominantly affected by the impingement and turning effects. In the second passage, heat transfer in $TR=0.16$ is slightly higher than that in $TR=0.07$ in reverse, mainly because after the turning effect, higher temperature ratio causes more severe density inhomogeneity in each cross-section. Thus, more complex air mixing happens in the downstream, resulting in a higher heat transfer.

## 4.2. Rotating results

Rotation effect, turn effect, and buoyancy parameter are the most important factors in heat transfer in a rotating two-pass rectangular channel with smooth walls. And the Coriolis force is known as the primary factor due to rotation. Compared to the stationary conditions, heat transfers in rotating channel increase in trailing surface and decrease in leading surface for the first radially outward passage, and the reverse is true for the second radially inward passage.

The conventional perspective of correlating heat transfer in rotating channel is to consider the variation of rotation number. However, from the definition of Buoyancy number ($Buo=(\Delta T/T)Ro^2(r/D)$), it is the combination of rotation number, radius ratio and wall temperature ratio. Therefore, it is more meaningful and comprehensive to find the correlation between heat transfer and Buoyancy number under different rotating conditions and wall heated conditions. There are three ways to alter the Buoyancy number: varying rotation number, varying wall temperature ratio and varying radius ratio. In the current study, experiments for

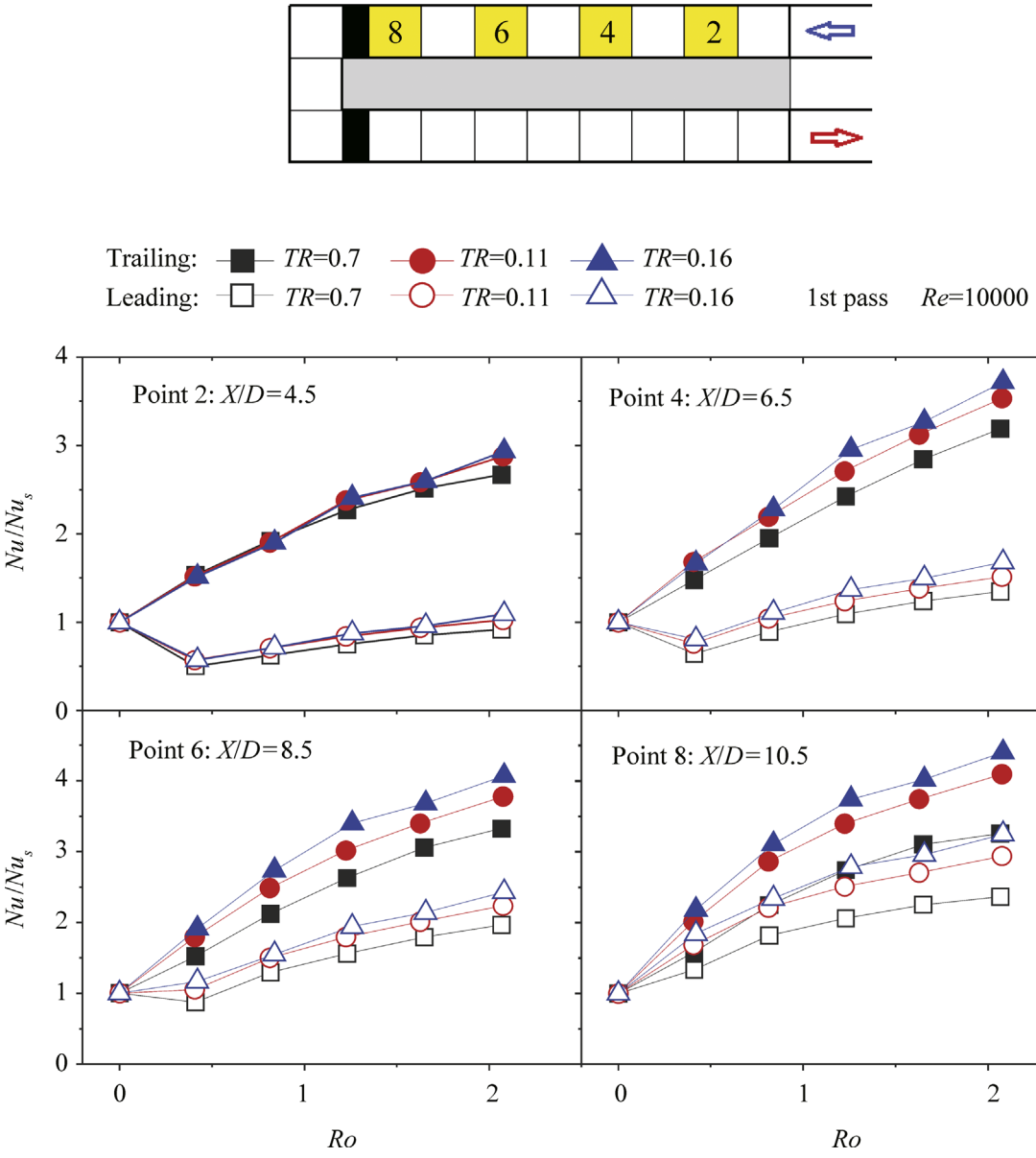


**Figure 11** Nusselt number ratio for different *TR* in the first pass.

different rotation numbers and wall temperature ratios are selected to correlate heat transfer and Buoyancy numbers.

*4.2.1. Varying rotation number*

Given the selected hydraulic diameter ($D_h$), different rotation numbers (*Ro*) are obtained by varying rotational speed or channel inlet velocity. And the different Buoyancy numbers (*Buo*) are obtained by varying rotation numbers or wall temperature ratios under the selected rotating radius ratio ($R_{ave}/D_h$). Figure 6 shows the ranges of *Ro* and *Buo* at different Reynolds numbers in current experiments. The highest *Ro* and *Buo* is 2.08 and 12.9 with rotation speed of 1000 rpm at $Re = 10000$, which covers the whole engine working conditions.

*4.2.1.1. Radial outward passage.* In the first radial outward flow passage, Nusselt number ratios are basically monotone increasing along with rotation number in trailing surface. This is mainly due to the trailing wall experiences higher velocity and colder fluid, which further enhances heat transfer. Also, the Coriolis induced secondary flow also enhances heat transfer on trailing surface. On the leading surface, Nusselt number ratios decrease when the rotation number is relatively low, and increase again after a critical rotation number on each *X/D* location. Phenomena are in the same tendency when Nusselt number ratios are in term of Buoyancy numbers, as is shown in Figure 7.

Due to fixed radius ratio, the extensive variation of Buoyancy number mainly attributes to the change of rotation number when the wall temperature ratio varies slightly at a given location. It is easily to recognize that as rotation number increases, the Coriolis and Buoyancy forces are enhanced simultaneously. When the Nusselt number ratios are put into the same surface with different

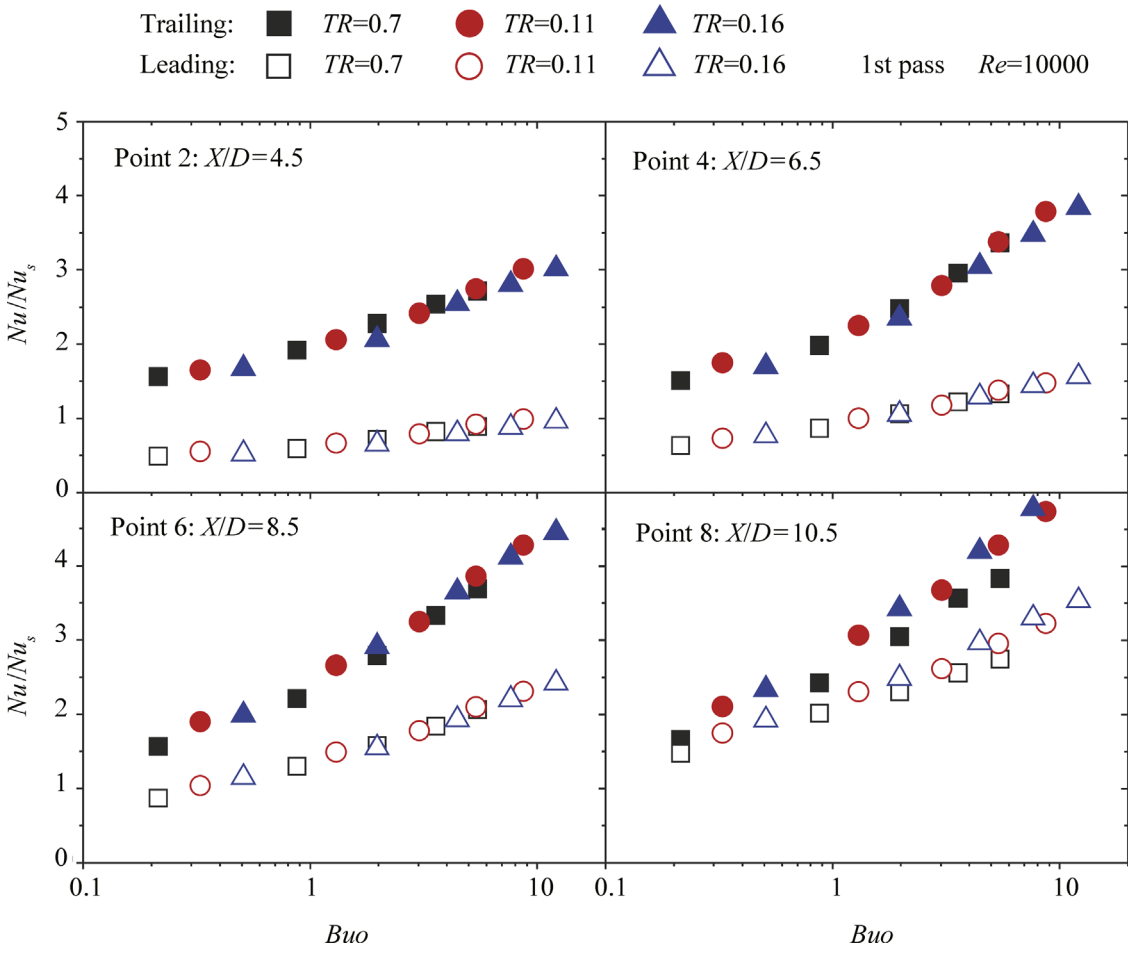


**Figure 12** Effect of Buoyancy number on Nusselt number ratios with different *TR* in the first pass.

*X*/*D* location, a critical Buoyancy number happens both on trailing and leading surface, as is shown in Figure 8. Interestingly, after the critical point, *Nu* ratio increase with Buoyancy number at different rate. This is mainly due to the different effect of Coriolis forces and centrifugal buoyancy force at different locations (*X*/*D*). The location near the 180-deg turn experiences stronger centrifugal buoyancy force. Also, the location near the entrance (*X*/*D*=4.5) is affected by channel entrance effect. But the entrance effect turns weaker as flow goes down-stream wise. Thus, stronger rotational effect is experience at point 8 (*X*/*D*=10.5).

Nusselt number ratios slightly increase before the critical Buoyancy number for each *X*/*D* location on trailing surface, and then separate into different increase rate. For leading surface, Nusselt number ratios are almost the constant value for each *X*/*D* location before the critical Buoyancy number, and then separate into different increase rate as the trailing surface does. It means that the effect of Buoyancy number on heat transfer is limited before the critical Buoyancy number in the first passage for both trailing and leading surface.

*4.2.1.2. Radial inward passage.* In the radial inward passage, heat transfer on leading surface is expected to be higher than trailing surface due to Coriolis force of bulk flow directs to the leading edge. Figure 9 shows the effect of Buoyancy number on Nusselt number ratios at each location in the second passage. At high rotation numbers and their corresponding Buoyancy numbers, heat transfer on trailing surface will exceed the leading surface due to the unstable double flow peaks occurred near the trailing surface. And the exceed-point of Buoyancy number gets smaller as the *X*/*D* location gets larger (*X*/*D*=18.6, $Buo_{ex}$=3.06; *X*/*D*=20.6, $Buo_{ex}$=2.42).

When the Buoyancy number is relatively low, the buoyancy effect is not so apparent and heat transfer on both surface changes slightly for each *X*/*D* location in the second passage. The critical Buoyancy number also happens on both trailing and leading surface, after which heat transfer shows different increase rate, as is shown in Figure 10. This critical point for each surface is the same with the first outward channel, which is the beginning point of the Buoyancy effect.

Given the same radius ratio and wall temperature ratio, varying rotation number will change Buoyancy number simultaneously. And the relationships between heat transfer and Buoyancy number are in accord with those obtained under rotation number. However, when varying wall temperature ratio, the combined effects of rotation number

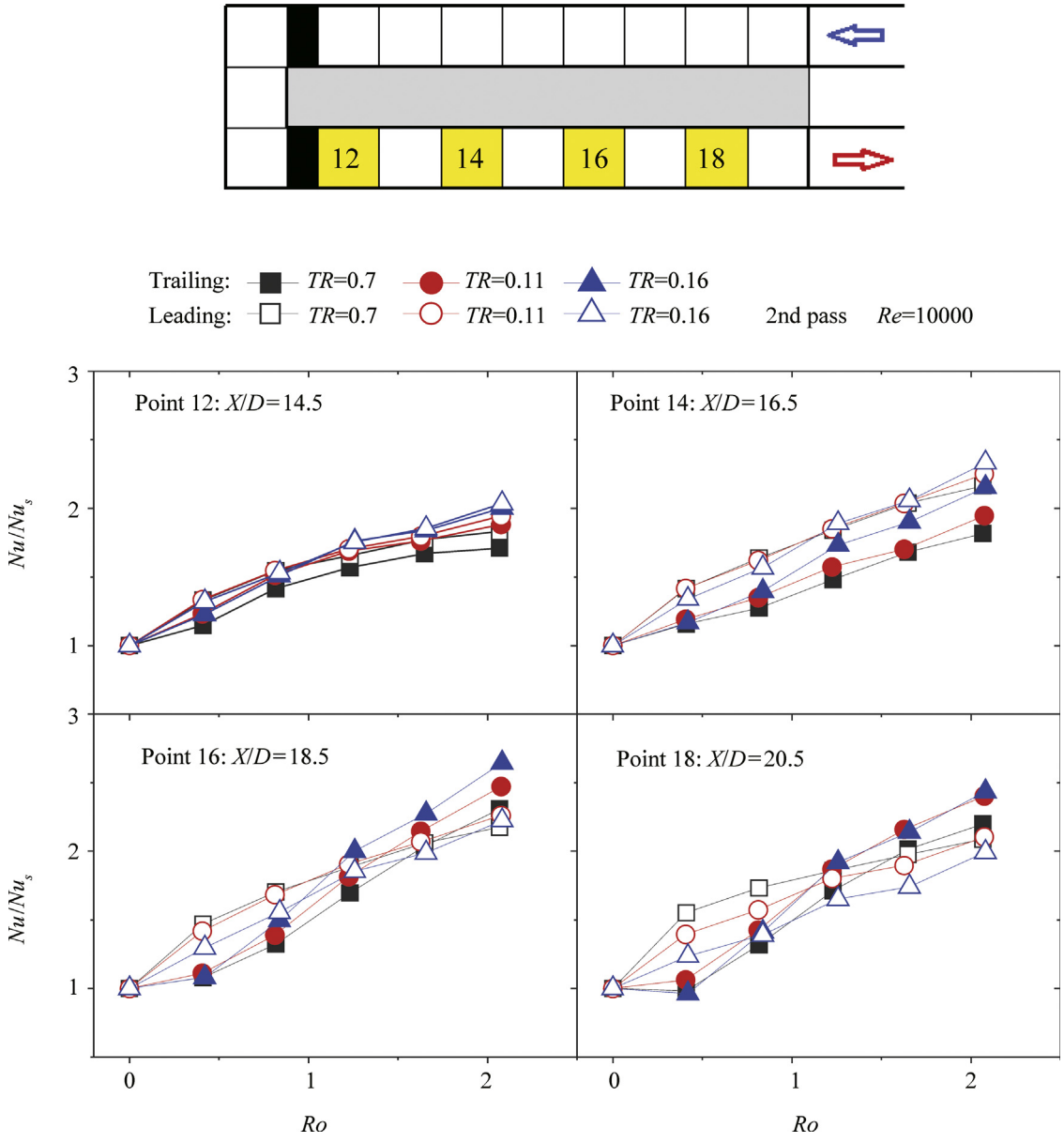


**Figure 13** Nusselt number ratio for different *TR* in the first pass.

and wall temperature ratio are much more complex and the advantage of using Buoyancy number to correlate heat transfer will be more obvious.

*4.2.2. Varying wall heating temperature ratios*

In rotating internal cooling channel, varying inlet density ratio is performed by varying wall temperature ratio, and is another way to change the Buoyancy numbers. Given the same rotation number, the increasing wall temperature ratio will affect the heat transfer ratio on both trailing and leading surfaces. As the rotation number increase, the interaction of Coriolis force and buoyancy force is so dominant in the entire cooling channel that their coupled influences are hard to be separated. Thus, it is necessary to conduct detailed study to find the effect of Buoyancy effect induced by different wall temperature ratio at high rotation number.

*4.2.2.1. Radial outward passage.* Figure 11 shows the effect of wall temperature ratio on the leading and trailing surface Nusselt number ratio for the rotation number studied between 0 and 2.08. In this radial outward passage, the buoyancy force near both leading and trailing surface directs to the rotating axis. Due to the interaction of strong Coriolis force and buoyancy force, heat transfer increase on both leading and trailing surface for different *TR* states. For leading surface, as the rotation number has exceeded critical rotation number, the fluid near wall flows reverse which acts the same direction with the buoyancy force. Thus, a larger *TR* condition along with stronger buoyancy force definitely enhances heat transfer on leading surface. However, for each cross-section, due to the reverse flow part occurs near the leading wall, a larger flow mass will balance the cross-section mass continuity, and thus, more coolant flow on the trailing surface resulting in higher

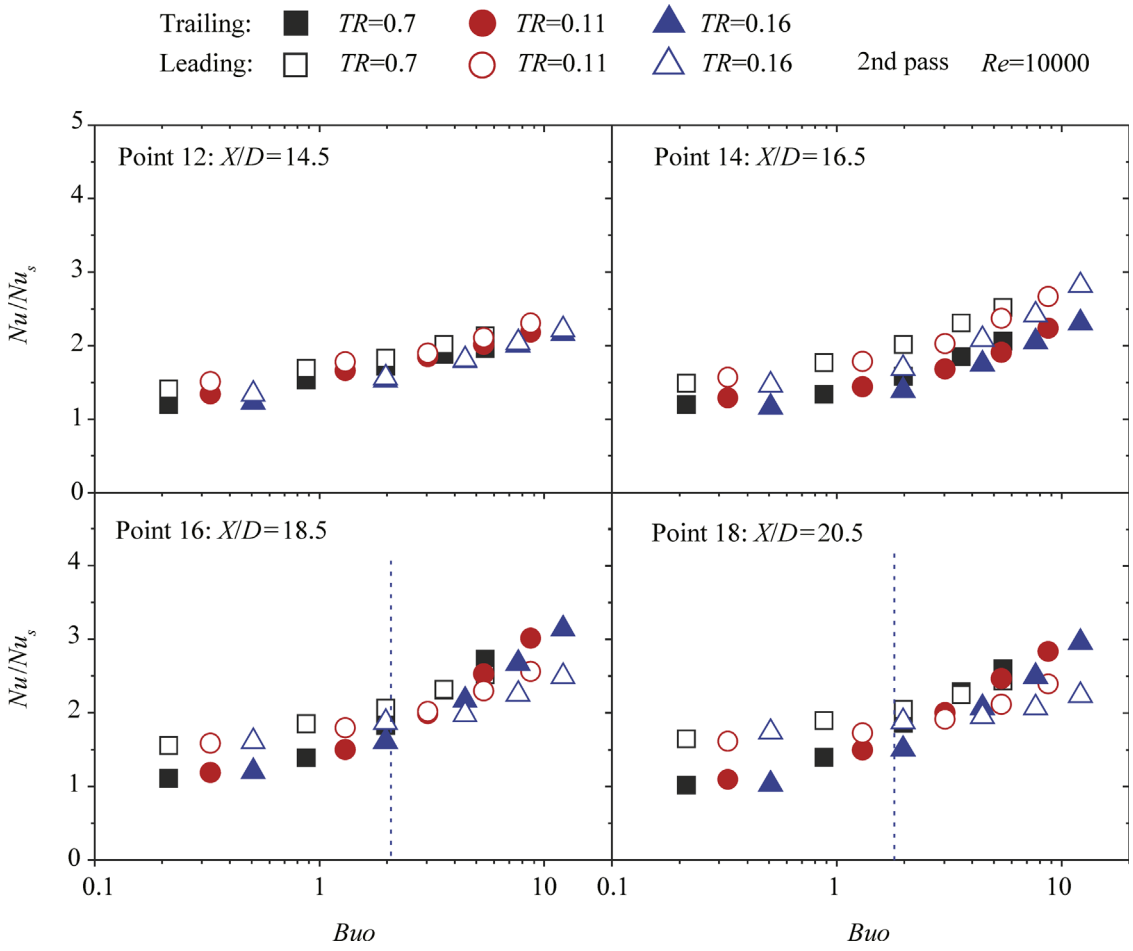


**Figure 14** Effect of Buoyancy number on Nusselt number ratios with different *TR* in the second pass.

heat transfer. Therefore, though the larger *TR* condition cause stronger buoyancy force which will weaken heat transfer on trailing surface, the strong flow shift will offset this negative influence and in reverse enhances heat transfer on trailing surface.

Figure 12 shows the effect of Buoyancy number on Nusselt number ratios with different *TR* (*TR*=0.07, 0.11, 0.16) in the first passage. The heat transfer tendency is in accord with that obtained by varying rotation number. It means that Buoyancy number is appropriate to evaluate the combined effect of rotation number and wall temperature ratio on heat transfer.

*4.2.2.2. Radial inward passage.* In the radial inward passage, the buoyancy force directs to the rotating axis which enhance heat transfer on both leading and trailing surface. Thus, the larger *TR* condition along with the stronger buoyancy force causes higher heat transfer, as is shown in Figure 13. When the rotation number is relatively high, the buoyancy effect becomes prominent and a double peek velocity profile occurs in the second passage. This makes the trailing wall to be an unstable suction side, and flow separation is possibly generated, causing higher heat transfer on trailing surface than on leading surface. The larger *TR* condition, the lower rotation number is needed for heat transfer on trailing surface to exceed the leading surface. It is obvious that the stronger buoyancy effect promotes heat transfer enhancement at the same rotation number condition.

The Correlation between heat transfer and Buoyancy number for different *TR* in the second passage is shown in Figure 14. It is surprisingly to find that the exceed-point of Buoyancy number comes to the same for different *TR*. As the rotation number is relatively low and *TR* is relatively high, the effect of higher *TR* makes up some part of rotational effect, and thus, higher heat transfer are observed.

Given the same rotation number, the increasing wall temperature ratio causes the heat transfer ratio to increase on both trailing and leading surfaces. And the Buoyancy number is the combined parameter of these two influential factors. Thus, it is better to correlate heat transfer with Buoyancy number when different *TR* conditions are considered. And the critical exceed-point happens in the second passage can be made to the same Buoyancy number.

## 5. Conclusions

This study experimentally investigated heat transfer in rotating smooth square U-duct. The effects of Buoyancy

number on heat transfer are discussed. Due to the experimental results, the conclusions can be drawn as follow:

(1) **Non-rotating results:** heat transfer in higher *TR* condition is weaker than lower *TR* condition in the first pass, but is slightly higher in the second pass after the 180-deg turn effect.
(2) **High rotation number effect:** when the rotation number keeps enhancing, there are critical points on the suction surface for both two passages. In the first pass, heat transfer on the leading surface increase after the critical rotation number. While in the second pass, heat transfer on the trailing surface exceeds the leading surface.
(3) **Rotation induced Buoyancy effect:** given the same radius ratio and wall temperature ratio, varying rotation number will change Buoyancy number simultaneously. Thus, the relationships between heat transfer and Buoyancy numbers are in accord with those obtained under different rotation numbers. For both leading and trailing surface, a critical Buoyancy number exists for each *X/D* location. Before the critical point, the effect of Buoyancy number on heat transfer is limited; but after that, the Nusselt number ratios show different increase rate.
(4) **Wall temperature ratio induced Buoyancy effect:** given the same rotation number, higher wall temperature ratios with its corresponding higher Buoyancy numbers substantially enhance heat transfer on both passages. The heat transfer tendency obtained at different Buoyancy numbers is in accord with that obtained by varying rotation numbers. And the critical exceed-point that heat transfer from trailing surface higher than leading surface happens at the same Buoyancy number for different wall temperature ratios in the second passage. Thus, the stronger buoyancy effect promotes heat transfer enhancement at high rotation number condition.

## Acknowledgements

The authors would like to express their acknowledgement to AVIC Commercial Aircraft Engine Co., Ltd. for the financial support.

## References

[1] J.C. Han, S. Dutta, S.V. Ekkad, Gas Turbine Heat Transfer and Cooling Technology, Taylor and Francis, New York, 2000, 1–646.
[2] J.C. Han, Turbine blade cooling studies at Texas A&M University: 1980–2004, Journal of Thermo-Physics and Heat Transfer 20 (2) (2006) 161–187.
[3] J.C. Han, M. Huh, Recent studies in turbine blade internal cooling, Heat Transfer Research 41 (8) (2010) 803–828.
[4] J.C. Han, P.R. Chandra, S.C. Lau, Local heat/mass transfer in distributions around sharp 180° turns in two-pass smooth and rib roughened channels, ASME Journal of Heat Transfer 110 (1988) 91–98.
[5] W.J. Yang, N. Zhang, J. Chiou, Local heat transfer in a rotating serpentine flow passage, ASME Journal of Heat Transfer 114 (1992) 354–361.
[6] S. Mochizuki, J. Takamura, S. Yamawaki, W.J. Yang, Heat transfer in serpentine flow passages with rotation, ASME Journal of Turbomachinery 116 (1994) 321–330.
[7] B.V. Johnson, J.H. Wagner, G.D. Steuber, F.C. Yeh, Heat transfer in rotating serpentine passages with selected model orientations for smooth or skewed trip walls, ASME Journal of Turbomachinery 116 (1994) 738–744.
[8] M. Huh, J. Lei, Y.H. Liu, J.C. Han, High rotation number effect on heat transfer in a rectangular ($AR$=2:1) two-pass channel, ASME Paper GT2009-59421, 2009.
[9] M. Huh, J. Lei, J.C. Han, Influence of channel orientation on heat transfer in a two-pass smooth and ribbed rectangular channel ($AR$=2:1) under large rotation numbers, ASME Paper GT2010-22190, 2010.
[10] G.S. Azad, M.J. Uddin, J.C. Han, H.K. Moon, B. Glezer, Heat transfer in a two-pass rectangular rotating channel with 45° angled rib turbulators, ASME Journal of Turbomachinery 124 (2002) 251–259.
[11] W.L. Fu, L.M. Wright, J.C. Han, Heat transfer in two pass rotating rectangular channels ($AR$=1:2 and $AR$=1:4) with smooth walls, ASME Journal of Heat Transfer 127 (3) (2005) 265–277.
[12] L.M. Wright, W.L. Fu, J.C. Han, Influence of entrance geometry on heat transfer in rotating rectangular cooling channels ($AR$=4:1) with angled ribs, ASME Journal of Heat Transfer 127 (4) (2005) 378–387.
[13] J.H. Wagner, B.V. Johnson, T.J. Hajek, Heat transfer in rotating passage with smooth walls and radial outward flow, ASME Journal of Turbomachinery 113 (1991) 42–51.
[14] J.H. Wagner, B.V. Johnson, F. Kopper, Heat transfer in rotating serpentine passage with smooth walls, ASME Journal of Turbomachinery 113 (1991) 321–330.
[15] H.W. Deng, L. Qiu, Z. Tao, S.Q. Tian, Heat transfer study in rotating smooth square U-duct at high rotation numbers, International Journal of Heat and Mass Transfer 66 (2013) 733–744.
[16] T.J. Hajek, J.H. Wagner, B.V. Johnson, Coolant passage heat transfer with rotation, Lewis Research Center, Turbine Engine Hot Section Technology, NASA N89-17314, 1986.
[17] L. Qiu, H.W. Deng, J.N. Sun, Z. Tao, S.Q. Tian, Pressure drop and heat transfer in rotating smooth square U-duct under high rotation numbers, International Journal of Heat transfer and Mass Transfer 66 (2013) 543–552.
[18] S.J. Kline, F.A. McClintock, Describing uncertainty in single simple experiments, Mechanical Engineering 75 (1953) 3–8.